Polymer Chemistry

Accepted Manuscript

ROYAL SOCIETY OF CHEMISTRY

www.rsc.org/polymers

Polymer Chemistry

PAPER

Construction of regio- and stereoregular poly(enaminone)s by multicomponent tandem polymerizations of diynes, diaroyl chloride and primary amines†

Received 00th January 20xx,
Accepted 00th January 20xx

DOI: 10.1039/x0xx00000x

www.rsc.org/

Haiqin Deng,[ab] Rongrong Hu,[ac] Anakin C. S. Leung,[ab] Engui Zhao,[ab] Jacky W. Y. Lam,*[ab] and Ben Zhong Tang*[abc]

Polyhydroaminations for the synthesis of stable nitrogen-substituted conjugated polymers with well-defined structures remains to be a great challenge and the control of the regio- and stereochemistry of the enamine product of the hydroamination is non-trivial. Herein we report an efficient tandem polymerization of alkynes, carbonyl chloride and primary amines to afford regio- and stereoregular conjugated poly(enaminone)s. The atom-economical one-pot sequential polycoupling-hydroamination polymerization catalyzed by $Pd(PPh_3)_2Cl_2$/CuI proceeded smoothly under mild conditions, furnishing nitrogen-substituted conjugated polymers with high molecular weights (up to 46 100) and high regio-/stereoregularities (100%) in nearly quantitative yields (up to 99%). Single crystal structure of the model compound, together with the NMR spectra comparison of model compound and polymers gave a direct insight into the stereoselectivity of the polymerization, verifying the sole *Z*-vinylene isomer of the polymers. Through the exquisite structural design strategy of the intramolecular hydrogen bond of the resultant hydroamination product, the tautomerization between enamine and imine as well as *E*/*Z* isomerization was successfully avoided, providing products with high chemical stability and sole *Z*-vinylene isomers. The conjugated polymers display excellent solubility in common organic solvents, good film-forming ability, and high thermal stability. The hydrogen bond formation of the polymer helps blocking the potential photo-induced electron transfer process and the polymer shows unique aggregation-enhanced emission phenomenon: their solutions are weakly emissive, while their nanoaggregates or thin films are brightly emissive. Furthermore, thin films of the polymers enjoy high refractive indices (1.9103–1.6582) in a wide wavelength region of 400–1000 nm, which can be further modulated by UV irradiation. Meanwhile, well-resolved fluorescent photopatterns of the polymers can be fabricated through the UV irradiation of thin films via a copper photomask.

Introduction

Construction of functional macromolecules is of great academic significance and technological implication, which has attracted much attention among scientists.[1] As an important branch, heteroatom-containing conjugated polymers are in great demand in many potential high-tech applications, attributed to their unique electronic and photophysical properties.[2] Various polymerization methods towards heteroatom-containing conjugated polymers have been developed over the past decades, and hetero-elements such as sulfur, oxygen, nitrogen, silicon, are normally incorporated into the polymer structures.[3] However, the exploration of facile polymerization methodologies to afford regio- and stereo-regular products remains challenging.[4]

Among many polymerization approaches, hydroelement addition reactions of alkynes are considered to be one of the most efficient methods to construct conjugated polymers with σ–π conjugation (Scheme 1).[5] Some frontier work about polyhydroelement additions has been reported. For example, linear and hyperbranched poly(silylenevinylene)s were synthesized by polyhydrosilylations of alkynes and silanes.[6] Furthermore, polyhydrothiolations of aromatic diynes and dithiols catalyzed by rhodium complexes,[7] and catalyst-free polyhydrothiolations were reported,[8] which proceeded smoothly in a regioselective manner, affording conjugated poly(vinylene sulfide)s. In the reported polyhydrosilylations and polyhydrothiolations, despite that high stereoselectivity were reported in some cases,[6] both *Z*-vinylene and *E*-vinylene isomers were generally observed in the obtained polymers.

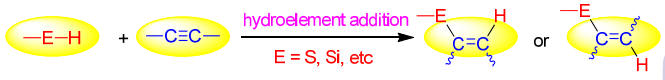

Scheme 1 Hydroelement additions of alkynes.

[a] Department of Chemistry, Institute for Advanced Study, Institute of Molecular Functional Materials, Division of Biomedical Engineering, Division of Life Science and State Key Laboratory of Molecular Neuroscience, The Hong Kong University of Science & Technology (HKUST), Clear Water Bay, Kowloon, Hong Kong.
[b] HKUST-Shenzhen Research Institute, No. 9 Yuexing 1st RD, South Area, Hi-tech Park, Nanshan, Shenzhen 518057, China.
[c] Guangdong Innovative Research Team, SCUT-HKUST Joint Research Laboratory, State Key Laboratory of Luminescent Materials and Devices, South China University of Technology (SCUT), Guangzhou 510640, China.

† Electronic Supplementary Information (ESI) available: crystal data and structure refinement for model compound **4**; frontier orbital theory for the PET effect; quantum yields of **4** and P**1a**–**b**/**2**/**3a**–**b** in solution and aggregate state. See DOI: 10.1039/b000000x/

Polyhydroaminations with direct addition of amines to alkynes, however, are rarely reported, probably due to the poor stability of the addition product. Of the reported small molecular hydroamination reactions,[9] therein lies one critical issue which limits the development of hydroaminations. As shown in Scheme 2, the tautomerization between enamine and imine easily takes place, and the C=N bond in imine is unstable which can be decomposed.[10] Meanwhile, the stereoselectivity of the newly formed C=CH bond is difficult to control. It is thus a great challenge to synthesize nitrogen-substituted conjugated polymers with well-defined structures through polyhydroaminations.

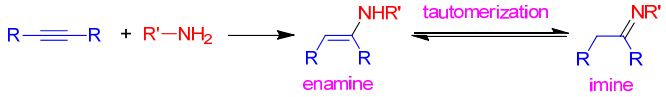

Scheme 2 Hydroamination reaction and enamine-imine tautomerization.

To develop polymerization methods with operational simplicity, synthetic efficiency, high atom economy, and environmental benefit, scientists have made great endeavor to investigate multicomponent polymerizations (MCPs),[11] including the MCPs of alkynes, aldehydes and amines,[12] and the MCPs of alkynes, azides and amines/alcohols.[13] In our previous work, multicomponent tandem polymerizations (MCTPs) with maximization of the reaction efficiency and atom-/step-economy have been developed, which include sequential or cascade reaction processes. For example, a one-pot, three-component, coupling-hydrothiolation-cyclocondensation MCTP of alkyne, aroyl chloride, and ethyl 2-mercaptoacetate was explored as a powerful tool for the preparation of conjugated poly(arylene thiophenylene) with structural regularity, processability and advanced functionality.[14] To explore the general applicability of this MCTP, the one-pot, two-step, three-component coupling-addition tandem polymerization of alkyne, aroyl chloride, and common aliphatic/aromatic thiols are investigated, demonstrating an efficient polymerization method to access sulfur-substituted conjugated polymers.[15]

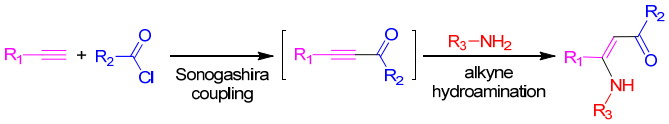

Scheme 3 One-pot enaminone syntheses by coupling-addition of alkynes, aroyl chlorides and primary amines.

Encouraged by the successful development of MCTPs of alkyne, aroyl chloride, and thiols through combining Sonogashira coupling and hydrothiolation, it is promising to extend this concept by using amines instead of thiols to develop sequential coupling-hydroamination polymerizations. In fact, Müller et al. reported an economical and practical protocol of one-pot three-component coupling-addition sequential reaction of alkyne, carbonyl chloride and primary amine, using $Pd(PPh_3)_2Cl_2$/CuI as catalyst to afford enaminone with high efficiency, endowing sole *Z*-isomer product due to the formation of intramolecular hydrogen bond (Scheme 3).[16] The six-member ring linked by the intramolecular hydrogen bond between N–H and C=O groups can help to stabilize the *Z*-vinylene structure, avoiding tautomerization between enamine and imine and *E*/*Z* isomerization, inducing high stereoselectivity, and hence providing perfect solution to the unsolved problems of polyhydroaminations.

In this work, a one-pot three-component coupling-hydroamination sequential polymerization was developed to afford nitrogen-substituted conjugated polymers with regio- and stereoregular structures. Tetraphenylethene (TPE) was incorporated into the monomer structures because it is a well-known aggregation-induced emission (AIE) fluorophores.[17] The restriction of intramolecular motion was proposed as the main reason for the AIE effect of TPE derivatives.[18] In solution, the phenyl rings can rotate via the single-bond axes, which serves as a relaxation channel for the decay of excitons, rendering the TPE molecules nonemissive. In the aggregated state, however, such rotation is physically restricted, blocking the nonradiative decay pathway, which enables the molecules with bright emission. The introduction of TPE units may thus endow the polymers with aggregation-enhanced emission (AEE) feature. The bulky and twisted structure of TPE units can also prevent close intermolecular interactions, which presumably benefits the solubility of the resultant polymers. The sequential polymerizations of TPE-containing diynes (**1a**–**b**), diaroyl chloride (**2**) and primary amines (**3a**–**b**) (Scheme 4) can proceed smoothly to furnish stereospecific conjugated polymers (P**1a**–**b**/**2**/**3a**–**b**) with satisfactory molecular weights (M_w) in nearly quantitative yields. The resultant polymers possess good chemical stability, excellent solubility, good thermal stability, aggregation-enhanced emission, high light refractivity, as well as photopatternability.

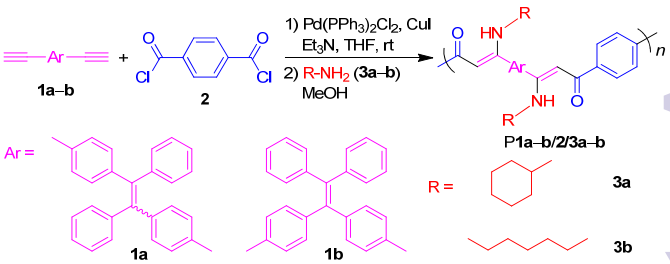

Scheme 4 Polymerizations of diynes **1a**–**b**, carbonyl chloride **2**, and primary amines **3a**–**b**.

Results and discussion

Polymerization

To develop the one-pot three-component sequential coupling-hydroamination reaction into an efficient polymerization approach for the preparation of conjugated poly(enaminone)s, monomers with multiple functional groups were designed. TPE-containing diynes **1a**–**b** were prepared according to our previous publications.[19] Commercially available terephthaloyl chloride **2** and primary amines **3a–b** were chosen as the other two monomers. The typical polymerization was carried out in THF under nitrogen in the presence of $Pd(PPh_3)_2Cl_2$, CuI and triethylamine (Et_3N). Diyne **1a–b** was first reacted with dicarbonyl chloride **2** for 15 min at room temperature, **3a–b** were then added with methanol to proceed the hydroamination reaction, affording nitrogen-substituted conjugated polymers (Scheme 4).

Temperature effect of the hydroamination was first evaluated with the polymerization of **1a**, **2**, and **3a** as shown in

Table 1. The polymerization was first carried out at room temperature for 6 h, only trace amount of target polymer was obtained. Prolonging the reaction time to 14 h did not improve the polymerization and few desired polymeric product was generated in the system. Reaction temperature of hydroamination was then increased to 80 °C. After 6 h polymerization, polymer with high M_w of 40 800 was obtained in a high yield of 99%. High temperature is hence necessary for the hydroamination process and further optimizations of the polymerization were carried out at 80 °C.

Table 1 Temperature effect on the polymerization of **1a**, **2** and **3a**[a]

no.	T (°C)	t (h)	yield (%)	M_w[b]	M_w/M_n[b]
1[c]	25	6	/		
2[c]	25	14	/		
3	80	6	99	40 800	2.3

[a]Carried out in THF under nitrogen in the presence of $Pd(PPh_3)_2Cl_2$, CuI and Et_3N. [**1a**] = 0.05 M, [**2**] = 0.05 M, [**3a**] = 0.20 M, [Pd] = 4 mol%, [Cu] = 8 mol%, [Et_3N] = 0.10 M. Monomer **1a** was reacted with **2** for 15 min at room temperature prior to the addition of **3a**. [b]Determined by GPC in THF on the basis of a linear polystyrene calibration. [c]Undesired polymeric products were obtained.

Solvent effect of the polymerization was then systematically investigated (Table 2). Of the tested solvents including DCM, DMF, toluene, and THF, THF presents the most suitable medium for the polymerization, giving a soluble polymeric product with the highest M_w and yield (Table 2, no. 4). Satisfactory result was also obtained in toluene with high M_w of 30 400, low polydispersity (M_w/M_n = 1.4), and a high yield of 97%. However, only trace amount of polymeric product was produced in DCM or DMF, indicating strong solvent effect of the polymerization.

Table 2 Solvent effect on the polymerization of **1a**, **2** and **3a**[a]

no.	solvents	yield (%)	M_w[b]	M_w/M_n[b]
1	DCM/methanol	trace		
2	DMF/methanol	trace		
3	toluene/methanol	97	30 400	1.4
4[c]	THF/methanol	99	40 800	2.3

[a]Carried out in the solvents under nitrogen at 80 °C in the presence of $Pd(PPh_3)_2Cl_2$, CuI and Et_3N. [**1a**] = 0.05 M, [**2**] = 0.05 M, [**3a**] = 0.20 M, [Pd] = 4 mol%, [Cu] = 8 mol%, [Et_3N] = 0.10 M. Monomer **1a** was reacted with **2** for 15 min at room temperature prior to the addition of **3a**, DMF = dimethyl formamide. [b]Determined by GPC in THF on the basis of a linear polystyrene calibration. [c]Data taken from Table 1, no. 3.

Reaction time of the hydroamination after the addition of **3a** and methanol was then tested in THF. As shown in Table 3, the polymerization is very efficient. In general, with the second step reaction time ranging from 2 to 24 h, the yields of P**1a**/**2**/**3a** were excellent which remained almost constant (~ 98%), and the M_w values of the polymers were generally larger than 36 000. The polymers obtained from 12 h and 24 h became partially soluble in common organic solvents.

Table 3 Time course on the polymerization of **1a**, **2** and **3a**[a]

no.	t (h)	yield (%)	S[b]	M_w[c]	M_w/M_n[c]
1	2	99	√	36 400	2.3
2	4	99	√	46 100	2.9
3[d]	6	99	√	40 800	2.3
4	12	99	Δ	42 100	3.0
5	24	98	Δ	41 800	3.2

[a]Carried out in THF under nitrogen at 80 °C in the presence of $Pd(PPh_3)_2Cl_2$, CuI and Et_3N. [**1a**] = 0.05 M, [**2**] = 0.05 M, [**3a**] = 0.20 M, [Pd] = 4 mol%, [Cu] = 8 mol%, [Et_3N] = 0.10 M. Monomer **1a** was reacted with **2** for 15 min at room temperature prior to the addition of **3a**. [b]*S* = solubility tested in common organic solvents such as THF, DCM, and chloroform: √ = completely soluble and Δ = partially soluble. [c]Determined by GPC in THF on the basis of a linear polystyrene calibration. [d]Data taken from Table 1, no. 3.

The influence of the monomer concentrations on the polymerization was also investigated (Table 4). When the concentrations of **1a** and **2** were both 0.10 M, insoluble gel was rapidly formed within 2 h. The concentrations of **1a** and **2** were then decreased to 0.08 M, while keeping [**1a**]:[**2**]:[**3a**] = 1:1:4, partially soluble polymer was produced in high yield. The best polymerization result was achieved with a monomer concentration of 0.05 M. Further dilution of the monomers to 0.02 M led to dramatically decreased yield and M_w.

Table 4 Monomer concentration on the polymerization of **1a**, **2** and **3a**[a]

no.	[**1a**] (M)	t (h)	yield (%)	S[b]	M_w[c]	M_w/M_n[c]
1	0.10	2	gel			
2	0.08	6	96	Δ	20 200	2.5
3[d]	0.05	6	99	√	40 800	2.3
4	0.02	6	43	√	13 400	2.3

[a]Carried out in THF under nitrogen at 80 °C in the presence of $Pd(PPh_3)_2Cl_2$, CuI and Et_3N for 6 h. [**2**] = [**1a**], [**3a**] = 4 [**1a**], [Et_3N] = 2 [**1a**], [Pd] = 4 mol%, [Cu] = 8 mol%. Monomer **1a** was reacted with **2** for 15 min at room temperature prior to the addition of **3a**. [b]*S* = solubility tested in common organic solvents such as THF, DCM, and chloroform: √ = completely soluble and Δ = partially soluble. [c]Determined by GPC in THF on the basis of a linear polystyrene calibration. [d]Data taken from Table 1, no. 3.

Last but not least, other monomer structures were tested under the optimum condition to explore the general applicability of this polymerization and the results were summarized in Table 5. All the polymerizations proceeded smoothly, affording polymers with high M_w (21 400–40 800) and low polydispersity (2.0–2.3) in high yields (95–99%). It's noteworthy that the polydispersity of the polymers obtained from this sequential polymerization is much smaller compared

with the previously reported polymers prepared by similar MCTPs.[14]

Table 5 Polymerization of **1a**–**b**, **2** and **3a**–**b**[a]

no.	monomer	yield (%)	M_w[b]	M_w/M_n[b]
1[c]	**1a/2/3a**	99	40 800	2.3
2	**1b/2/3a**	99	21 400	2.2
3	**1a/2/3b**	95	25 200	2.0

[a]Carried out in THF under nitrogen at 80 °C in the presence of $Pd(PPh_3)_2Cl_2$, CuI and Et_3N for 6 h. [**1a**] = [**1b**] = [**2**] = 0.05 M, [**3a**] = [**3b**] = 0.20 M, [Pd] = 4 mol%, [Cu] = 8 mol%, [Et_3N] = 0.10 M. Monomer **1a**/**1b** was reacted with **2** for 15 min at room temperature prior to the addition of **3a**/**3b**. [b]Determined by GPC in THF on the basis of a linear polystyrene calibration. [c]Data taken from Table 1, no. 3.

Model reaction

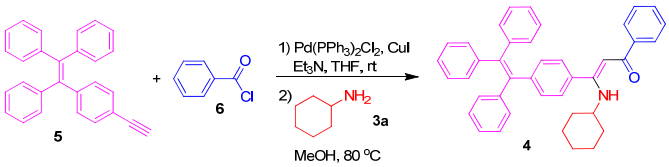

Scheme 5 Synthetic route to model compound **4**.

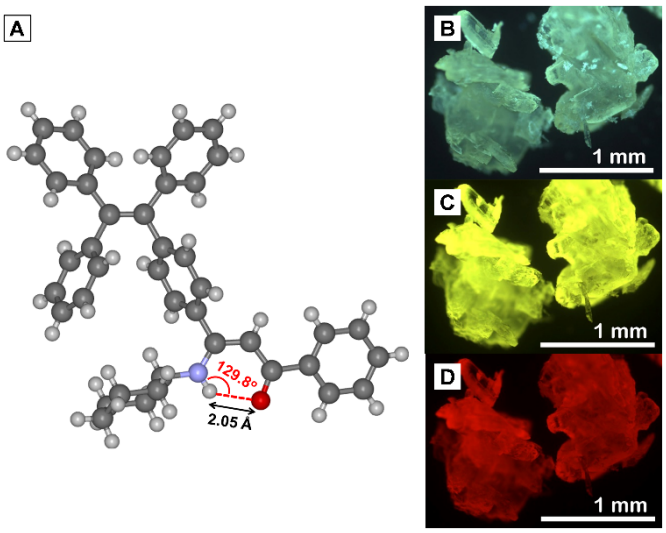

Fig. 1 (A) Single crystal structure (CCDC 1009262) and fluorescence images of 4 taken under a fluorescent microscope with excitation light of (B) 330–385 nm, (C) 460–490 nm, and (D) 510–560 nm.

Model compound was also prepared to assist the structural characterization of the polymers (Scheme 5). TPE-containing monoyne **5** was first reacted with benzoyl chloride **6**, catalyzed by $Pd(PPh_3)_2Cl_2$/CuI under nitrogen at room temperature for 3 h. The reactive intermediate obtained from the first step then directly underwent the next in-situ reaction at 80 °C after addition of **3a**, affording model compound **4**. To provide direct insight into the molecular structure, single crystals were obtained from the hexane/DCM solution of **4**. From the X-ray analysis shown in Fig. 1A and Table S1, *Z* isomer of the newly formed C=C bond was obtained exclusively with the formation of intramolecular hydrogen bond between N–H and O=C groups. In addition, the crystals are observed to emit green, yellow and red fluorescence under UV, blue, and green light irradiation of the fluorescent microscope, respectively (Fig. 1B–D). Upon irradiation of different excitation light, the emission light with wavelength smaller than the excitation light wavelength, was eliminated by specific filters. Hence different fluorescence of model compound **4** was observed.

Structural Characterization

All the monomers, model compound and polymers were characterized by standard spectroscopic techniques, which provided satisfactory analysis data corresponding to the expected molecular structures (see Experimental Section). For example, the IR spectra of **1a**, **2**, **3a**, **4** and P**1a/2/3a** were shown in Fig. 2 for comparison. The absorption bands of **1a** associated with ≡C–H and C≡C stretching vibrations were located at 3275 and 2106 cm^{-1}, respectively. Meanwhile, an absorption band with double peaks in the IR spectrum of **3a** was observed at 3348 and 3279 cm^{-1}, which was associated with the NH_2 stretching vibration. The bands were disappeared in both the spectra of **4** and P**1a/2/3a**, confirming that the terminal triple bonds and NH_2 groups have been completely consumed by the reaction.

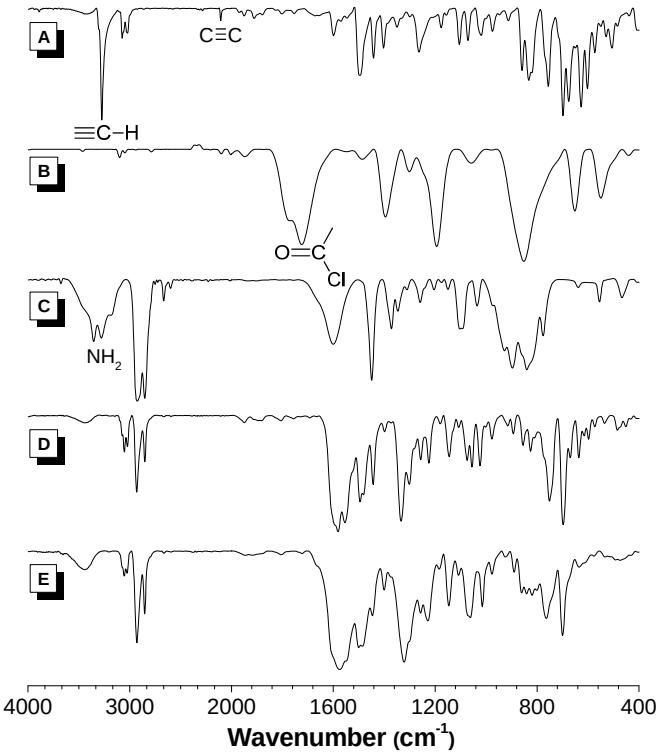

Fig. 2 IR spectra of (A) **1a**, (B) **2**, (C) **3a**, (D) **4** and (E) P**1a/2/3a**.

Furthermore, their ^1H NMR spectra were compared in Fig. 3. The resonance of acetylene proton of **1a** at δ 3.03 was disappeared in the spectra of **4** and P**1a/2/3a**. The resonances of the aromatic protons of **2** at δ 8.25 and the CH proton of **3** next to the NH_2 group at δ 2.40 shifted to δ 7.87 and δ 3.19, respectively, in the model compound and polymer after the reaction. On the other hand, new peaks emerged at δ 5.69 and δ 11.40 in the spectra of both **4** and P**1a/2/3a**, representing

the newly formed C=CH group next to the carbonyl group, and the N–H group, respectively. The N–H resonance was located at such a low field, indicating the formation of intramolecular hydrogen bond. Generally, the resonance peaks of P**1a/2/3a** are broader than those of **4**, suggesting its polymeric nature. Similarly, in the ^{13}C NMR spectra, the resonances of C≡C–H of **1** at δ 83.9 and 77.7 was absent in the spectra of **4** and P**1a/2/3a** (Fig. 4). The absorption of carbonyl group of **2** at δ 170.8 was shifted to δ 188.1 after the reaction. In the spectra of **4** and P**1a/2/3a**, two new peaks emerged at δ 166.1 and 93.4, which were associated with the =CAr(N) and =CH(COAr) olefin carbons, respectively. In addition, the newly formed olefin group was confirmed to be *Z*-isomer in **4** by X-ray single crystal structure analysis. From the above discussed ^{1}H/^{13}C NMR spectra, P**1a/2/3a** shares exactly the same NMR spectra pattern with **4**, without any additional peaks observed for the *E*-isomer, proving its highly regio- and stereospecific structure as shown in Scheme 4.

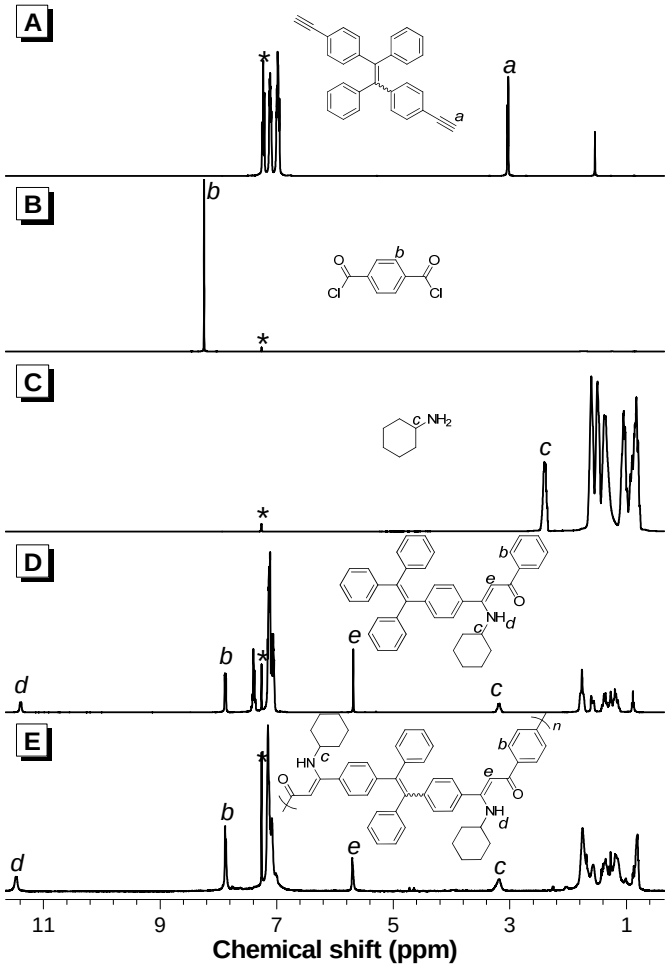

Fig. 3 ^{1}H NMR spectra of (A) **1a**, (B) **2**, (C) **3a**, (D) **4** and (E) P**1a/2/3a**.

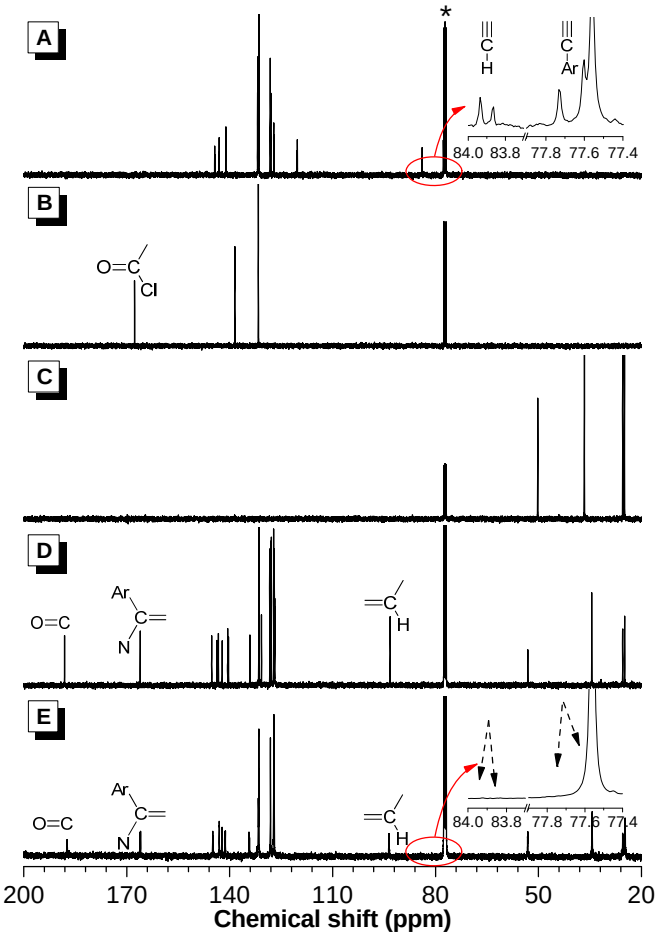

Fig. 4 ^{13}C NMR spectra of (A) **1a**, (B) **2**, (C) **3a**, (D) **4** and (E) P**1a/2/3a**.

Solubility and Thermal Stability

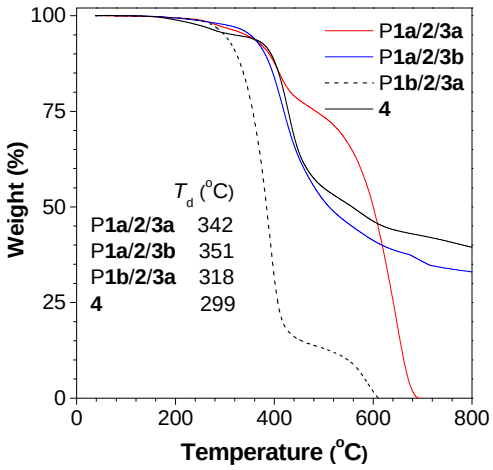

Fig. 5 TGA thermograms of **4** and P**1a**–**b/2/3a**–**b** recorded under nitrogen at a heating rate of 10 °C/ min.

Although the resulting polymers are composed of conjugated aromatic backbones, they possess good solubility in common organic solvents, such as THF, DCM, chloroform, etc. The introduction of TPE units into the polymer backbone played a major role in improving the solubility, owing to the bulky and twisted structure of TPE units, which may result in large

intermolecular distance and hence provide free volume for solvent molecules. Moreover, the polymers generally possess good film-forming ability and can be readily fabricated into thin films by spin-coating process. With their conjugated polymer backbones and aromatic components, the polymers enjoy good thermal stability. Their thermal properties were evaluated by Thermogravimetric analysis, indicating that the degradation temperatures (T_d) of P**1a**–**b**/**2**/**3a**–**b** at their 5% weight losses under nitrogen were in the range of 318–351 °C (Fig. 5).

Photophysical Properties

With the typical AIE-active TPE units embedded in the molecular skeletons, AIE or AEE characteristics can be expected from both model compound and the corresponding polymers. The photophysical properties of **4** and P**1a**/**2**/**3a** were hence systematically investigated. Absorption spectra of **4** and P**1a**/**2**/**3a** in pure THF solutions with a concentration of 10 μM were firstly measured as shown in Fig. 6. The absorption maxima of **4** and P**1a**/**2**/**3a** were located at 355 and 387 nm, respectively, indicating better conjugation in the polymer.

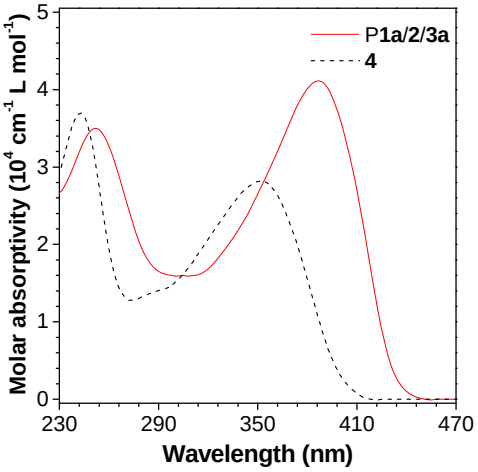

Fig. 6 Absorption spectra of **4** and P**1a**/**2**/**3a** in THF solutions. Solution concentration: 10 μM.

Both polymers and model compound are comprised of TPE as the fluorophore, which are linked with amine moieties, representing typical photo-induced electron transfer (PET) system (Fig. S1).[20] In the general PET process, when the fluorophore is irradiated, the electron on the highest occupied molecular orbital (HOMO) is excited to the lowest unoccupied molecular orbital (LUMO). If the HOMO level of the amine moiety with lone pair electrons is located between the LUMO and HOMO levels of the adjacent fluorophores, the electron on the HOMO level of the amine will be easily transferred to the HOMO level of the fluorophores. Such process hinders the returning of the electron on the LUMO level of the fluorophores to its HOMO level, and hence causes fluorescence quenching.[21] However, in **4** and P**1a**/**2**/**3a**, the potential PET process was blocked by the intramolecular hydrogen bond, rendering the fluorophores emissive.

The photoluminescence (PL) of both **4** and P**1a**/**2**/**3a** were estimated by a spectrofluorometer (Fig. 7 and 8). The THF solution of **4** was weakly emissive with a flat peak at 460 nm in its PL spectrum. The emission intensity slowly increased with the addition of water, a poor solvent of **4**, until 70 vol% of water was added. Eventually, the emission intensity increased by 8.9-fold when nanoaggregates formed in THF/water mixture with 99 vol% water content and the emission peak was red-shifted to 500 nm. The emission maximum of P**1a**/**2**/**3a** in THF solution was located at 536 nm, bathochromically shifted about 76 nm compared with that of **4**. In contrast to the small molecule, the fluorophores of polymer were covalently-linked in the polymer backbone, which partially restricted the free rotation of the phenyl rings to some extent in the solution. Thus the THF solution of P**1a**/**2**/**3a** was faintly emissive. The continuous addition of water into THF solution of P**1a**/**2**/**3a** with a constant concentration of 10 μM gradually enhanced its emission intensity without a noticeable shift in the emission peak. The highest emission intensity was observed in THF/water mixture with 70 vol% water and its intensity was about 3.0-fold higher than that of its THF solution, demonstrating aggregation-enhanced emission characteristics. When more water was added, the emission intensity decreased because of the poor solubility of P**1a**/**2**/**3a** in the aqueous mixtures.

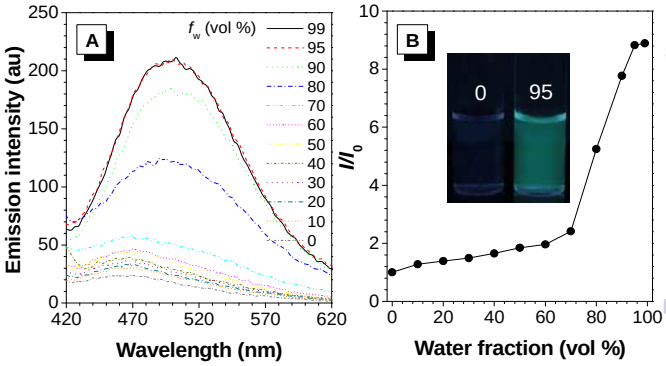

Fig. 7 (A) Emission spectra of **4** in THF/water mixtures with different water fractions (f_w). (B) Plot of relative emission intensity (I/I_0) versus the water fraction of the aqueous mixtures of **4**. Inset: Fluorescent photographs of **4** in THF solution and 95% aqueous mixture taken under 365 nm UV irradiation. Solution concentration: 10 μM; excitation wavelength: 355 nm.

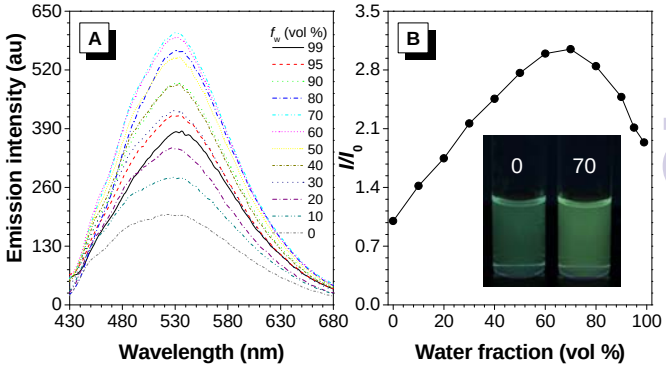

Fig. 8 (A) Emission spectra of P**1a**/**2**/**3a** in THF/water mixtures with different water fractions (f_w). (B) Plot of relative emission intensity (I/I_0) versus the water fraction of the aqueous mixtures of P**1a**/**2**/**3a**. Inset: Fluorescent photographs of P**1a**/**2**/**3a** in THF solution and 70% aqueous mixture taken under 365 nm UV irradiation. Solution concentration: 10 μM; excitation wavelength: 387 nm.

The fluorescence photographs of **4** and P**1a/2/3a** in THF and THF/water mixtures were displayed in the insets of Fig. 7B and 8B. With the identical dye concentration, THF solution of **4** was almost non-emissive and the nanoaggregates formed in THF/water mixture with 95 vol% water fraction were brightly emissive under UV irradiation. Similarly, the nanoaggregates of P**1a/2/3a** formed in THF/water mixture is more emissive compared with its THF solution. The PL study suggested that the formation of intramolecular hydrogen bond prevented the electron transfer from the HOMO level of amine group to the HOMO level of the TPE fluorophores. The quantum yields of **4** and P**1a-b/2/3a-b** were also measured in solution and aggregate state, respectively. The detailed information was summarized in Table S2, which further demonstrated their AIE and AEE characteristics.

Light Refraction

Processable macromolecules with high refractive indices (*n*) are promising candidates due to a variety of practical applications in advanced optoelectronic fabrications, such as lenses, prisms, substrates for advanced display devices, optical adhesives of organic light-emitting diode devices, and microlens components for charge coupled devices or complementary metal oxides, etc.[22] Generally, conventional organic polymer materials including polystyrenes, poly(methylmethacrylate)s, and polycarbonates possess refractive indices in the region of 1.49–1.58.[23] Usually, polymer materials with a large number of well-known contributors for increasing refractivity such as carbonyl groups, heteroatoms, and aromatic rings can be expected to display high refractivity. Polymers P**1a**–**b/2/3a**–**b** comprised plenty of carbonyl groups, heteroatoms, TPE moieties, and a conjugated polymer backbone. Hence, the thin films of P**1a/2/3a**, P**1a/2/3b**, and P**1b/2/3a** fabricated through spin-coating process exhibited high *n* values of 1.9103–1.6582, 1.9758–1.6501, and 2.0182–1.6403 in a wide spectral region of 400–1000 nm, respectively (Fig. 9A). Such high refractivity is presumably derived from both the special polymer structure and the TPE building blocks.

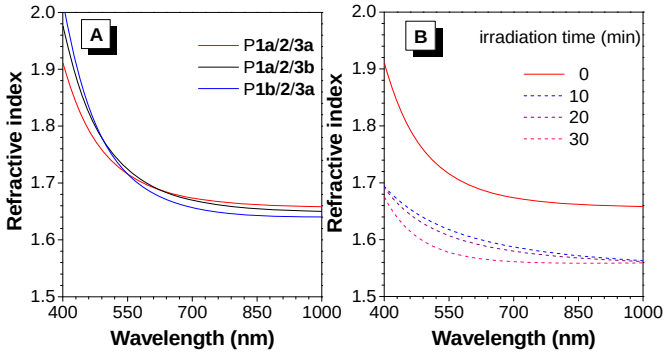

Fig. 9 Wavelength dependence of refractive indices of thin films of (A) P**1a**–**b/2/3a**–**b** and (B) P**1a/2/3a** with different UV irradiation time.

Modulation of refractive index is another critical technology in optical communication and optical data storage devices such as compact discs, digital versatile discs, blue ray discs, holographic recording materials, etc.[24] Therefore, it is of great importance to develop materials with high and facilely tunable refractive indices. P**1a/2/3a** was investigated as an example and the changes in the *n* values of its thin film with different UV irradiation time were shown in Fig. 9B. When UV irradiation was applied on the polymer thin film in air, photo-oxidation reaction occurred, which changed the chemical composites of the film and hence the *n* values. The *n* values dropped quickly in the same wavelength region upon the exposure of UV light. Particularly, after 30 min UV irradiation, the *n* values of the film decreased to 1.6746–1.5590 in the wavelength region of 400–1000 nm, and the difference of *n* value was about 0.1204 at 632.0 nm, demonstrating efficient refractivity modulation.

Fluorescent Photopatterning

It is highly desirable to fabricate fluorescent photopatterns for the constructions of photonic and electronic devices, biological sensing and probing systems.[25] Since the polymers exhibit good film-forming ability, photosensitivity, and high emission efficiency in the solid state, it is of great potential to fabricate them into luminescent photopatterns through photolithography. P**1a/2/3a** and P**1a/2/3b** were dissolved in 1,2-dichloroethane, respectively, to form emissive thin films on silicon wafers by spin-coating. Afterwards, the films were irradiated under UV light through a copper photomask for 20 min and two-dimensional patterns with high resolution and sharp edges were observed under a fluorescence microscope (Fig. 10). The fluorescence of the exposed region was quenched due to the photo-oxidation reaction in air.

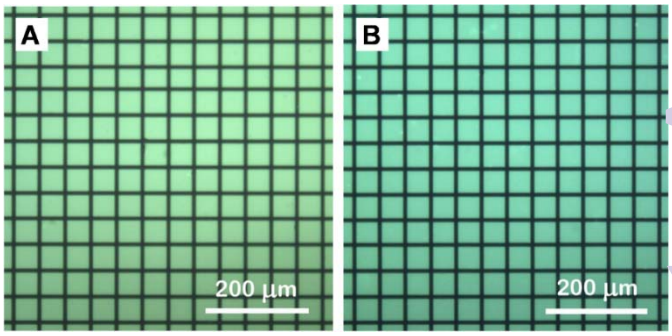

Fig. 10 Two-dimensional fluorescent photopatterns generated by photo-oxidation of thin films of (A) P**1a/2/3a** and (B) P**1a/2/3b**. The photographs were taken under UV light illumination (330–385 nm).

Conclusions

In this work, we have reported an efficient one-pot coupling-hydroamination polymerization of alkynes, carbonyl chlorides, and primary amines. The one-pot sequential Sonogashira coupling of alkyne and carbonyl chloride, and hydroamination of internal alkyne proceeded smoothly under mild conditions, furnishing nitrogen-containing conjugated polymers with high regioselectivity and stereoselectivity, high molecular weights in excellent yields. Through the design of intramolecular hydrogen bond formation between N–H and C=O groups in the product, 100% stereoselectivity of the newly formed olefin groups was achieved. Moreover, benefited by the hydrogen bond-bound six member ring, *Z*-isomer was stabilized, the transformation between *Z*-vinylene and *E*-vinylene was

blocked, and the enamine-imine tautomerization was inhibited. Most importantly, the intramolecular hydrogen bonds hampered the potential PET process and enabled the polymers showing aggregation-enhanced emission behaviors. The well-defined conjugated polymers enjoyed good solubility in common organic solvents, excellent film-forming ability, high thermal stability, large and tunable refractivity, photosensitivity, etc.

Through this efficient and convenient one-pot tandem polymerization approach towards functional conjugated polymer materials, polyhydroamination can be realized, overcoming the perennial problems such as the low efficiency, unstable product structure, poor regioselectivity and stereoselectivity, and tautomerization. We believe the general applicability of such efficient approach will pave the way to facile syntheses of heteroatoms-containing conjugated polymers with well-defined structures and multiple functionalities.

Experimental

Materials and methods

THF was distilled from sodium benzophenone ketyl under a nitrogen atmosphere prior to use. Terephthaloyl dichloride and Et_3N were purchased from Sigma-Aldrich. $Pd(PPh_3)_2Cl_2$, CuI and methanol were ordered from Zhejiang Metallurgical Research Institute Co., Ltd., International Laboratory USA, and Merck, respectively. All of them were used as received without further purification except special illustration. Diyne **1a**–**b** and monoyne **5** were prepared according to the literature procedures.[19]

^1H and ^{13}C NMR spectra were measured by a Bruker ARX 400 NMR spectrometer using $CDCl_3$ as solvent and tetramethylsilane (TMS; δ = 0 ppm) as internal standard. IR spectra were measured by a Perkin-Elmer 16 PC FT-IR spectrophotometer. High resolution mass spectra (HRMS) were evaluated on a GCT Premier CAB 048 mass spectrometer operated in MALDI-TOF mode. Single crystal X-ray diffraction data was collected at 100 K on a Bruker-Nonices Smart Apex CCD diffractometer with graphite monochromated Mo-Kα radiation. Analysis of the data was carried out through the SAINT and SADABS routines, and the structure and refinement were obtained employing the SHELTL suite of X-ray programs (version 6.10). The weight average molecular weights (M_w), number average molecular weights (M_n), and polydispersity indices (M_w/M_n) of the polymers were evaluated by a Waters Associates gel permeation chromatography (GPC) system equipped with a RI detector. Distilled THF was used as solvent to dissolve the polymers (~2 mg mL^{-1}). The solutions were filtered through 0.45 μm PTFE syringe-type filters before injected into the GPC system, and THF was used as the eluent in a flow rate of 1.0 mL min^{-1}. A set of linear polystyrenes standards (Waters) covering the M_w range of 10^3–10^7 were utilized for M_w and PDI calibration.

A Milton Roy Spectronic 3000 array spectrophotometer and a Perkin-Elmer LS 55 spectrofluorometer were utilized to record the UV-Vis absorption spectra and PL spectra, respectively. Quantum yields were determined by a calibrated integrating sphere. TGA was carried out under nitrogen on a Perkin-Elmer TGA 7 analyzer with a heating rate of 10 ^oC min^{-1}. Refractive indices were measured through a J. A. Woollam M-2000V multi-wavelength ellipsometer from 400 nm to 1000 nm. Photopatterning and refractivity modulation of the polymer film were conducted on a Spectroline ENF-280C/F UV lamp at a distance of 3 cm as light source with the incident light intensity of ~18.5 mW cm^{-2}. The films were prepared by spin-coating of the polymer solutions (10 mg polymer in 1 mL 1,2-dichloroethane) at 1000 rpm for 1 min on silicon wafers. The films were dried in a vacuum oven at room temperature overnight. The patterns were generated by UV irradiation on the film through copper photomask for 20 min. All of the photos were taken under a UV light source by an optical microscope (Olympus BX 41).

Polymerizations

All the polymerizations were carried out under nitrogen using a standard Schlenk technique. A typical procedure for the synthesis of P**1a**/**2**/**3a** from Table 1, no. 3 is given below as an example. A 25 mL Schlenk tube equipped with a magnetic stirrer was placed with TPE-containing diyne **1a** (76 mg, 0.20 mmol), terephthaloyl chloride **2** (41 mg, 0.20 mmol), $Pd(PPh_3)_2Cl_2$ (6 mg, 0.008 mmol), and CuI (3 mg, 0.016 mmol). The Schlenk tube was evacuated under vacuum and flushed with dry nitrogen for three times. 3.5 mL of THF and 0.06 mL of Et_3N was then injected and the resulting solution was stirred for 15 minutes at room temperature. Afterwards, cyclohexylamine **3a** (0.10 mL, 0.80 mmol) was injected with 0.50 mL of methanol (THF/methanol = 7/1). The reaction mixture was stirred for 6 h at 80 ^oC under nitrogen and was then added dropwise into 200 mL of methanol via a cotton filter to precipitate. The precipitate was allowed to stand overnight and collected by filtration. The polymer was washed with methanol and dried under vacuum at room temperature to a constant weight.

P**1a**/**2**/**3a**: Yellow powder; 99% (Table 1, no. 3). M_w: 40 800; M_w/M_n: 2.3 (GPC, polystyrene calibration). IR (KBr), υ (cm^{-1}): 3054, 3027, 2930, 2853, 1575, 1504, 1445, 1322, 1256, 1229. ^1H NMR (400 MHz, $CDCl_3$), δ (TMS, ppm): 11.47, 7.87, 7.15, 7.08, 5.69, 3.22, 1.75, 1.36, 1.15. ^{13}C NMR (100 MHz, $CDCl_3$), δ (TMS, ppm): 187.38, 166.17, 165.96, 144.93, 144.82, 143.04, 142.20, 141.43, 141.25, 134.36, 134.23, 131.65, 131.51, 128.11, 127.10, 93.60, 93.56, 53.16, 53.08, 34.45, 34.33, 25.46, 25.37, 24.83, 24.71.

P**1b**/**2**/**3a**: Yellow powder; 99% (Table 5, no. 2). M_w: 21 400; M_w/M_n: 2.2 (GPC, polystyrene calibration). IR (KBr), υ (cm^{-1}): 3054, 3027, 2930, 2853, 1575, 1504, 1445, 1400, 1322, 1258. ^1H NMR (400 MHz, $CDCl_3$), δ (TMS, ppm): 11.49, 7.88, 7.15, 7.06, 5.71, 3.20, 1.76, 1.36, 1.20. ^{13}C NMR (100 MHz, $CDCl_3$), δ (TMS, ppm): 187.40, 166.11, 144.63, 143.25, 142.22, 139.53, 134.28, 131.58, 131.49, 127.99, 127.20, 127.08, 93.55, 53.15, 34.44, 25.46, 24.81.

P**1a**/**2**/**3b**: Yellow powder; 95% (Table 5, no. 3). M_w: 25 200; M_w/M_n: 2.0 (GPC, polystyrene calibration). IR (KBr), υ (cm^{-1}): 3054, 3027, 2927, 2856, 1578, 1485, 1400, 1324, 1298, 1227. ^1H NMR (400 MHz, $CDCl_3$), δ (TMS, ppm): 11.43, 7.89, 7.15, 7.08, 5.73, 3.14, 1.53, 1.29, 0.88. ^{13}C NMR (100 MHz, $CDCl_3$), δ

(TMS, ppm): 187.75, 167.15, 145.09, 144.98, 143.04, 142.26, 141.40, 133.91, 131.53, 128.12, 127.35, 127.24, 127.11, 93.49, 44.98, 31.55, 30.97, 26.61, 22.72, 22.67, 14.24, 14.21.

Model Reaction

(*Z*)-3-(cyclohexylamino)-1-phenyl-3-(4-(1,2,2-triphenylvinyl)-phenyl)prop-2-en-1-one (**4**). Into a 25 mL Schlenk tube equipped with a magnetic stirrer was charged with TPE-containing monoyne (**5**) (178 mg, 0.50 mmol), benzoyl chloride (**6**) (0.06 mL, 0.50 mmol), $Pd(PPh_3)_2Cl_2$ (8 mg, 0.01 mmol), and CuI (4 mg, 0.02 mmol). 3.5 mL of THF and 0.08 mL of Et_3N was injected under nitrogen and then stirred at room temperature for 3 h. Cyclohexylamine **3a** (0.06 mL, 0.50 mmol) and 0.50 mL of methanol were injected subsequently by a syringe. The reaction mixture was further stirred for 24 h at 80 ^{o}C under nitrogen. 20 mL of water was added to quench the reaction and the solution was extracted with 30 mL of DCM for three times. The solvent was evaporated and the resultant crude product was purified by a silica-gel chromatography column using DCM/hexane (v/v 1/1) as the eluent to give light yellow solid in 72% yield. IR (KBr), υ (cm^{-1}): 3051, 3025, 2931. 2851, 1581, 1496, 1443, 1333, 1300, 1256, 1225. ^{1}H NMR (400 MHz, $CDCl_3$), δ (TMS, ppm): 11.40 (d, J = 9.3 Hz,1H), 7.88 (d, J = 6.4 Hz, 2H), 7.39 (m, 3H), 7.16–7.09 (m, 9H), 7.07–7.01 (m, 8H), 5.69 (s, 1H), 3.19 (d, J = 9.8 Hz, 1H), 1.77 (m, 4H), 1.38 (m, 2H), 1.21 (m, 4H). ^{13}C NMR (100 MHz, $CDCl_3$), δ (TMS, ppm): 188.12, 166.08, 145.27, 143.69, 143.42, 143.28, 142.19, 140.57, 140.36, 134.09, 131.56, 131.53, 131.48, 131.45, 130.74, 128.33, 128.03, 127.92, 127.89, 127.19, 127.04, 126.91, 126.89, 126.85, 93.25, 77.23, 53.11, 34.48, 25.49, 24.87. HRMS (MALDI-TOF): m/z 560.2910 [M + H^+, calcd 560.2953].

Preparation of Nanoaggregates

Stock THF solutions of **4** and P**1a**/**2**/**3a** with a concentration of 1 mM were prepared. Then 0.10 mL of the stock solutions were transferred to 10.00 mL volumetric flasks. After addition of appropriate amount of THF, water was added dropwise under vigorous stirring to prepare 10 μM THF/water mixtures with water fractions (f_w) of 0–99 vol%. The absorption and emission measurements of the resulting solutions were immediately performed.

Acknowledgements

This work has been partially supported by National Basic Research Program of China (973 Program; 2013CB834701), the University Grants Committee of Hong Kong (AoE/P-03/08), the National Science Foundation of China (21490570 and 21490574), the Research Grants Council of Hong Kong (604913 and 602212), Science and Technology Plan of Shenzhen (JCYJ20140425170011516) and Natural Science Fund of Guangdong Province (2014A030313659). B. Z. Tang thanks the support of the Guangdong Innovative Research Team Program (201101C0105067115).

Notes and references

1 P. C. Hiemenz and T. Lodge, *Polymer chemistry*, CRC Press, Boca Raton, 2007.
2 a) H. Sirringhaus, T. Kawase, R. H. Friend, T. Shimoda, M. Inbasekaran, W. Wu and E. P. Woo, *Science*, 2000, **290**, 2123–2126; b) D. T. McQuade, A. E. Pullen and T. M. Swager, *Chem. Rev.*, 2000, **100**, 2537–2574; c) C. L. Wang, H. L. Dong, W. P. Hu, Y. Q. Liu and D. B. Zhu, *Chem. Rev.*, 2012, **112**, 2208–2267; d) N. Wang, Z. Chen, W. Wei and Z. Jiang, *J. Am. Chem. Soc.*, 2013, **135**, 17060–17068; e) Z. Chen, P. Cai, J. Chen, X. Liu, L. Zhang, L. Lan, J. Peng, Y. Ma and Y. Cao, *Adv. Mater.*, 2014, **26**, 2586–2591; f) A. Facchetti, *Chem. Mater.*, 2011, **23**, 733–758.
3 a) J. Z. Liu, J. W. Y. Lam and B. Z. Tang, *Chem. Rev.*, 2009, **109**, 5799–5867; b) A. J. Qin, J. W. Y. Lam and B. Z. Tang, *Chem. Soc. Rev.*, 2010, **39**, 2522–2544; c) J. W. Y. Lam and B. Z. Tang, *Acc. Chem. Res.*, 2005, **38**, 745–754; d) K. Matyjaszewski and J. H. Xia, *Chem. Rev.*, 2001, **101**, 2921–2990; e) N. V. Tsarevsky and K. Matyjaszewski, *Chem. Rev.*, 2007, **107**, 2270–2299; f) N. Hadjichristidis, H. Iatrou, M. Pitsikalis and G. Sakellariou, *Chem. Rev.*, 2009, **109**, 5528–5578.
4 A. Molnar, A. Sarkany and M. Varga, *J. Mol. Catal. A: Chem.*, 2001, **173**, 185–221.
5 X. M. Zeng, *Chem. Rev.*, 2013, **113**, 6864–6900.
6 a) P. Lu, J. W. Y. Lam, J. Liu, C. K. W. Jim, W. Yuan, C. Y. K. Chan, N. Xie, Q. Hu, K. K. L. Cheuk and B. Z. Tang, *Macromolecules*, 2011, **44**, 5977–5986; b) P. Lu, J. W. Y. Lam, J. Z. Liu, C. K. W. Jim, W. Z. Yuan, N. Xie, Y. C. Zhong, Q. Hu, K. S. Wong, K. K. L. Cheuk and B. Z. Tang, *Macromol. Rapid Commun.*, 2010, **31**, 834–839; c) Z. J. Zhao, T. Jiang, Y. J. Guo, L. Y. Ding, B. R. He, Z. F. Chang, J. W. Y. Lam, J. Z. Liu, C. Y. K. Chan, P. Lu, L. W. Xu, H. Y. Qiu and B. Z. Tang, *J. Polym. Sci., Part A: Polym. Chem.*, 2012, **50**, 2265–2274.
7 a) J. Liu, J. W. Y. Lam, C. K. W. Jim, J. C. Y. Ng, J. Shi, H. Su, K. F. Yeung, Y. Hong, M. Faisal, Y. Yu, K. S. Wong and B. Z. Tang, *Macromolecules*, 2011, **44**, 68–79; b) B. C. Yao, J. Z. Sun, A. J. Qin and B. Z. Tang, *Chin. Sci. Bull.*, 2013, **58**, 2711–2718.
8 a) C. K. W. Jim, A. Qin, J. W. Y. Lam, F. Mahtab, Y. Yu and B. Z. Tang, *Adv. Funct. Mater.*, 2010, **20**, 1319–1328; b) B. C. Yao, J. Mei, J. Li, J. Wang, H. Q. Wu, J. Z. Sun, A. J. Qin and B. Z. Tang, *Macromolecules*, 2014, **47**, 1325–1333.
9 a) S. L. Shi and S. L. Buchwald, *Nat. Chem*, 2015, **7**, 38–44; b) F. Pohlki and S. Doye, *Chem. Soc. Rev.*, 2003, **32**, 104–114; c) R. Severin and S. Doye, *Chem. Soc. Rev.*, 2007, **36**, 1407–1420; d) T. E. Muller, K. C. Hultzsch, M. Yus, F. Foubelo and M. Tada, *Chem. Rev.*, 2008, **108**, 3795–3892.
10 a) M. L. Buil, M. A. Esteruelas, A. M. Lopez and A. C. Mateo, *Organometallics*, 2006, **25**, 4079–4089; b) M. A. Esteruelas, A. M. Lopez, A. C. Mateo and E. Onate, *Organometallics*, 2006, **25**, 1448–1460; c) N. T. Patil and V. Singh, *J. Organomet. Chem.*, 2011, **696**, 419–432.
11 a) Y. Z. Wang, X. X. Deng, L. Li, Z. L. Li, F. S. Du and Z. C. Li, *Polym. Chem.*, 2013, **4**, 444–448; b) X. X. Deng, Y. Cui, F. S. Du and Z. C. Li, *Polym. Chem.*, 2014, **5**, 3316–3320; c) A. Sehlinger, P. K. Dannecker, O. Kreye and M. A. R. Meier, *Macromolecules*, 2014, **47**, 2774–2783.
12 C. Y. K. Chan, N. W. Tseng, J. W. Y. Lam, J. Z. Liu, R. T. K. Kwok and B. Z. Tang, *Macromolecules*, 2013, **46**, 3246–3256.
13 I. H. Lee, H. Kim and T. L. Choi, *J. Am. Chem. Soc.*, 2013, **135**, 3760–3763; b) H. Kim and T. L. Choi, *ACS Macro. Lett.*, 2014, **3**, 791–794.
14 H. Q. Deng, R. R. Hu, E. G. Zhao, C. Y. K. Chan, J. W. Y. Lam and B. Z. Tang, *Macromolecules*, 2014, **47**, 4920–4929.
15 C. Zheng, H. Q. Deng, Z. J. Zhao, A. J. Qin, R. R. Hu and B. Z. Tang, *Macromolecules*, 2015, **48**, 1941–1951
16 A. S. Karpov and T. J. J. Muller, *Synthesis*, 2003, **18**, 2815–2826.

17 a) Y. N. Hong, J. W. Y. Lam and B. Z. Tang, *Chem. Commun.*, 2009, **29**, 4332–4353; b) R. Hu, N. L. Leung and B. Z. Tang, *Chem. Soc. Rev.*, 2014, **43**, 4494–4562.
18 a) B. Z. Tang and A. Qin, *Aggregation-induced emission : fundamentals*, 2013; b) Y. N. Hong, J. W. Y. Lam and B. Z. Tang, *Chem. Soc. Rev.*, 2011, **40**, 5361–5388; c) J. Mei, Y. Hong, J. W. Lam, A. Qin, Y. Tang and B. Z. Tang, *Adv. Mater.*, 2014, **26**, 5429–5479; d) J. D. Luo, Z. L. Xie, J. W. Y. Lam, L. Cheng, H. Y. Chen, C. F. Qiu, H. S. Kwok, X. W. Zhan, Y. Q. Liu, D. B. Zhu and B. Z. Tang, *Chem. Commun.*, 2001, **18**, 1740–1741.
19 a) R. Hu, J. L. Maldonado, M. Rodriguez, C. Deng, C. K. W. Jim, J. W. Y. Lam, M. M. F. Yuen, G. Ramos-Ortiz and B. Z. Tang, *J. Mater. Chem.*, 2012, **22**, 232–240; b) R. Hu, J. W. Y. Lam, M. Li, H. Q. Deng, J. Li and B. Z. Tang, *J. Polym. Sci., Part A: Polym. Chem.*, 2013, **51**, 4752–4764; c) Y. J. Liu, M. Gao, J. W. Y. Lam, R. R. Hu and B. Z. Tang, *Macromolecules*, 2014, **47**, 4908–4919.
20 M. T. Z. Spence and I. D. Johnson, *The molecular probes handbook: a guide to fluorescent probes and labeling technologies*, Live Technologies Corporation, Carlsbad, CA, 2010.
21 a) W. Zhang, Z. Ma, L. Du and M. Li, *Analyst*, 2014, **139**, 2641–2649; b) A. P. de Silva, T. S. Moody and G. D. Wright, *The Analyst*, 2009, **134**, 2385–2393.
22 a) T. Nakamura, H. Fujii, N. Juni and N. Tsutsumi, *Opt. Rev.*, 2006, **13**, 104–110; b) J. L. Regolini, D. Benoit and P. Morin, *Microelectron. Reliab.*, 2007, **47**, 739–742; c) D. W. Mosley, K. Auld, D. Conner, J. Gregory, X. Q. Liu, A. Pedicini, D. Thorsen, M. Wills, G. Khanarian and E. S. Simon, *Proc. Spie.*, 2008, **6910**, 691017–691018; d) J. Liu and M. Ueda, *J. Mater. Chem.*, 2009, **19**, 8907–8919.
23 a) J. Brandrup, E. H. Immergut and E. A. Grulke, *Polymer handbook, 4th edition*, Wiley, New York; Chichester, 2004; b) J. E. Mark, *Polymer data handbook*, Oxford University Press, Oxford; New York, 2009.
24 a) H. G. Unger, *Planar optical waveguides and fibres*, Clarendon Press, Oxford Eng.; New York, 1977; b) V. V. Krongauz and A. D. Trifunac, *Processes in photoreactive polymers*, Chapman & Hall, New York, 1995; c) T. Griesser, T. Höfler, G. Jakopic, M. Belzik, W. Kern and G. Trimmel, *J. Mater. Chem.*, 2009, **19**, 4557–4565; d) M. Edler, S. Mayrbrugger, A. Fian, G. Trimmel, S. Radl, W. Kern and T. Griesser, *J. Mater. Chem. C*, 2013, **1**, 3931–3938.
25 a) M. Irie, T. Fukaminato, T. Sasaki, N. Tamai and T. Kawai, *Nature*, 2002, **420**, 759–760; b) R. Ando, H. Mizuno and A. Miyawaki, *Science*, 2004, **306**, 1370–1373; c) J. M. Kim, Y. B. Lee, D. H. Yang, J. S. Lee, G. S. Lee and D. J. Ahn, *J. Am. Chem. Soc.*, 2005, **127**, 17580–17581; d) S. J. Lim, J. Seo and S. Y. Park, *J. Am. Chem. Soc.*, 2006, **128**, 14542–14547; e) M. S. Hahn, J. S. Miller and J. L. West, *Adv. Mater.*, 2006, **18**, 2679–2684; f) J. M. Kim, *Macromol. Rapid Commun.*, 2007, **28**, 1191–1212; g) Z. a. Li, Z. Jiang, S. Ye, C. K. W. Jim, G. Yu, Y. Liu, J. Qin, B. Z. Tang and Z. Li, *J. Mater. Chem.*, 2011, **21**, 14663–14671.

